PRICES SUBJECT TO CHANGE

Reproduced by
NATIONAL TECHNICAL
INFORMATION SERVICE
US Department of Commerce
Springfield, VA. 22151

JET PROPULSION LABORATORY

CALIFORNIA INSTITUTE OF TECHNOLOGY

PASADENA, CALIFORNIA

(NASA-CR-139358) PRELIMINARY REPORT ON PARABOLOIDAL REFLECTOR ANTENNA WIND TUNNEL TESTS (Jet Propulsion Lab.) 49 p

N74-75393

Unclas
16959

30/99

RE-ORDER NO. 62-709

INTERNAL MEMORANDUM

JPL CP-3

PRELIMINARY REPORT ON PARABOLOIDAL REFLECTOR ANTENNA WIND TUNNEL TESTS

Norman L. Fox
Bain Dayman, Jr.

Robert E. Covey

Robert E. Covey, Chief
Aerodynamic Facilities Section
Section 373

Copy No. _____
This document consists
of cover and 47 leaves.

JET PROPULSION LABORATORY
California Institute of Technology
Pasadena, California
February 28, 1962

1 - 47

CONTENTS

I. Introduction 1

II. Test Description 2

III. Discussion of Results 4

A. Reynolds Number Effects 4

B. Tunnel Floor and Support Interference Effects 5

C. Reflector Focal Length (Paraboloidal Depth) 6

D. Angular Rotation Center Location 7

E. Effects of Pitch Angle on Moments and Forces 7

F. Uniformly Distributed Porosity 7

G. Rim Porosity 8

H. Spoilers 8

I. Reflector Support Structure 9

J. Complete Configuration 10

K. Pressure Distribution 10

L. Dynamic Oscillation Data 11

Summary 11

References 12

Bibliography 13

Nomenclature 16

FIGURES

1. Antenna dishes of various depths (photograph)
2. Perforated antenna dishes (photograph)
3 Enlarged counterweight side surfaces pylon mounted (photograph)
4. Cowl-ring spoiler (photograph)
5. Fence-type spoiler (photograph)
6. Surface roughness on convex side of reflector (photograph)
7. Reynolds number comparison (drag coefficient vs Reynolds number for simple shapes)
8. Effect of Reynolds number on yaw moment (yaw moment coefficient vs yaw angle)
9. Comparison of side force with lift (side force or lift coefficient vs yaw or pitch angle)
10. Effect of antenna dish depth on yaw moment (yaw moment coefficient vs yaw angle)
11. Effect of yaw axis location on yaw moment (yaw moment coefficient vs yaw angle)
12. Effect of elevation angle on yaw moment (yaw moment coefficient vs yaw angle)
13. Effect of antenna dish uniform porosity (axial force coefficient vs yaw angle)
14. Effect of antenna dish uniform porosity on yaw moment (yaw moment coefficient vs yaw angle)

FIGURES (Cont'd)

15. Effect of antenna dish rim porosity on yaw moment (yaw moment coefficient vs yaw angle)

16. Effect of antenna dish spoilers on yaw moment (yaw moment coefficient vs yaw angle)

17. Effect of simulated structural support on yaw moment (yaw moment coefficient vs yaw angle)

18. Effect of simulated structural support on lateral force (lateral force coefficient vs yaw angle)

19. Effect of simulated structural support on axial force (axial force coefficient vs yaw angle)

20. 25% porosity pressure model (photograph)

21. Pressure distribution (polar plot of ΔC_p, concave side facing into wind)

22. Pressure distribution (polar plot of ΔC_p, convex side facing into wind)

RECORD No. 62-709

ABSTRACT

This paper presents some of the more significant results of a wind tunnel test on small models of paraboloidal reflector antennas. As contrasted to tests of a single final design configuration, the effects on wind loads of such parameters as focal distance to diameter ratio, surface porosity, spoilers, a simulated support structure, pivot center position, etc., were examined on relatively simple models. Evidence is offered to show that the Reynolds number of the test data is sufficiently high to make the results applicable to full-scale installations. The results of this test show some of the gains to be made by designing such an installation from wind loads, as well as structural and RF efficiency aspects. An annotated Bibliography presenting references on wind load tests on such antennas is also included.

I. INTRODUCTION

One of several interrelated problems in the design of a paraboloidal reflector directional antenna is wind loads (see Ref. 1.) These wind loads can not only distort the necessarily highly accurate shape of the antenna reflecting surface, but can create large torques which must be overcome by any angular positioning gear and have been known to cause structural damage. A large antenna of this nature, designed for tracking orbital and interplanetary flights, is particularly sensitive to wind loads in that it should be capable of use during critical phases of the trajectories in spite of adverse wind conditions.

Although a number of paraboloidal reflector antennas of various sizes, descriptions, and design purposes are in use, a surprisingly small amount of wind load data is available. What information is available, either from small model tests or field tests of existing installations, contains features which make it nearly impossible to form the comparisons necessary for optimization or design use. In order to obtain a consistent set of data showing the effect of parameters such as focal length to diameter ratio, distribution and amount of reflector surface porosity, devices to reduce loads, etc., a wind tunnel test program was embarked upon. Configurations were chosen for investigation which appeared to be reasonable compromises between aerodynamic loads, structural feasibility, and radio frequency performance.

Throughout this paper, conventional United States aerodynamic terminology and conventions are used. For the convenience of those not familiar with this terminology, the table of nomenclature at the end of this paper gives several

equivalent terms and some typical values. Except as noted, all data presented in this paper are in the stability axes system, with the moment center at the vertex of the paraboloidal reflecting surface.

II. TEST DESCRIPTION

These tests were performed in the Northrop Subsonic Wind Tunnel, which has a test section 7 ft high by 10 ft wide. All configurations tested incorporated 18-in.-diam. paraboloidal reflectors. Larger size models would have increased the distortion in the tunnel air flow to the level where the applicability of the resulting reduced data to field installations would be questionable. These paraboloidal reflectors were spin-formed from commercial copper sheet 1/8 in. thick. Several were perforated with 3/8-in.-diam. holes in reasonably uniform patterns to obtain the desired porosities. They were mounted near the tunnel floor at the center of the 20-ft-long test section. A 1-5/8-in.-diam. staff, which was shielded from wind loads by a 2-in.-diam. tube, connected the model to the large, accurate balance located below the floor. A "knuckle" at the top of this staff permitted pitch-angle settings from 0° to 180° in 5° increments. The models (and balance) were rotated by remote control to any desired yaw angle over a range in excess of 0° to 180°.

Major emphasis was placed on force and moment data. In addition, limited amounts of other types of data were obtained, such as:

1. Pressure distributions on three of the configurations.
2. Dynamic data, indicative of the severity of aerodynamically forced oscillations as a function of reflector attitude.

7

3. Photographs of tufts attached to several models, indicative of the air flow patterns responsible for the previously mentioned data.

The tunnel variables for this test were:

1. Wind velocity (Reynolds number) 85 to 260 mph, at atmospheric pressure, producing Reynolds numbers, based on model diameter, between 1.2 and 3.6 x 10^6.
2. Tunnel floor boundary layer thickness of 3 and 18 in., the latter approximating the terrestrial wind boundary layer relative to the model.
3. Clearance between the tunnel floor (simulated ground plane) and the bottom of the reflector surface of 1.56 and 6.61 in.

The various model configurations tested included the following variables:

1. Paraboloidal reflector focal length to diameter ratios of 0.25, 0.33, 0.42, and infinity (flat plate), corresponding to depth of diameter ratios of 0.250, 0.189, 0.149, and 0 (see Fig. 1.)
2. Paraboloidal reflector surface uniformly distributed porosities* of 0%, 10%, 25%, and 50% (see Fig. 2.)
3. Paraboloidal reflector surface outer edge porosities of 25% and 50% over the outer 10% and 25% of the reflector radius (see Fig. 3.)
4. Four protuberance-type spoilers (see Fig. 4 and 5.)

*The center 4-in. diam. of all configurations was distorted for mounting purposes and could not be perforated (see Fig. 4.)

5. Simulated reflector support structure with three sizes of counterweight side surface areas (aerodynamic balances) (see Fig. 3.)
6. A pylon (conical build-up on the 2-in.-diam. windshield) (see Fig. 3.)
7. Surface roughness on the back of the reflecting surface, 1-1/2% of the reflector diameter in height (see Fig. 6.)

In all cases, the reflecting surface was thin compared to its diameter, i.e., the case of an enclosed support structure was not examined.

Only a representative number of the above combinations was tested, and the pitch-angle range examined for a number of these combinations was very sparse. The test program included sufficient pertinent combinations to make it possible to estimate the performance of untested combinations by applying mutual differences, interpolation, and extrapolation.

III. DISCUSSION OF RESULTS

A. Reynolds Number Effects

One of the problems in applying the results from small-scale wind tunnel tests to full-scale installations is that of Reynolds number (scaling effects.) As shown by Fig. 7, in certain regions of Reynolds number, the nondimensional forces (and probably moments) can vary by a factor as great as five. Because such Reynolds number sensitivity data were virtually nonexistent for paraboloidal geometries, it was necessary to assume that the data represented by Fig. 7, based on spheres, cylinders, and flat plates, would be approximately applicable.

9

Based on this evidence that the model test Reynolds number would be in excess of the critical region, the test program was initiated.

During the course of the test, the Reynolds number was varied by a factor of three on one solid reflector configuration, and a factor of 1.35 on one porous reflector configuration. For the solid configuration, the yaw moment comparison is shown in Fig. 8 to demonstrate the lack of this scale effect. Except for these Reynolds number checks, the entire test was carried out at a Reynolds number, based on paraboloidal reflector diameter, of 2.7×10^6. This resulted from a tunnel air stream velocity of 192 mi/hr at sea level ambient pressure (a dynamic pressure of 95 lb/ft^2.)

B. Tunnel Floor and Support Interference Effects

If there were no ground plane (tunnel floor) air flow restraint, velocity nonuniformity (tunnel floor boundary layer), or support (windshield) interference, the model would have axial symmetry. Such a symmetrical model would show several identities in the resulting data. One of these comparisons is presented in Fig. 9, showing side force and lift force coefficients vs yaw and pitch angles, respectively (in wind axis orientation.) The discrepancies between these two curves must, then, be due to one or more of the above itemized factors.

The comparisons outlined in the above paragraph facilitate interpolation and extrapolation of the data resulting from this test. This feature is important in specific cases:

1. Data were obtained at a very limited number of pitch angles on all except one configuration.

10

2. Due to the manner in which the balance was used for resolving the forces and moments, the pitch and roll moment data are substantially inferior to the other four components.

Another support interference phenomenon may be seen in the resulting data. The presence of the pylon shown in Fig. 3, which represents a profile area of approximately 10% of the reflector frontal area, increases the moments approximately 10% and the forces approximately 5%.

C. Reflector Focal Length (Paraboloidal Depth)

Figure 10 shows the changes in the yaw moment coefficient as a function of the yaw angle for the various reflector focal length to diameter ratios. This figure shows that the deepest reflector exhibits approximately 20% higher yaw moment positive-peak (about the parabola vertex) than the shallowest reflector; however, the yaw moment negative-peak, while smaller in absolute magnitude than the positive moment, is greater for the shallower reflectors. There is relatively little change in the maximum rate of change of yaw moment with yaw angle.

It is interesting to note the yaw moment vs yaw angle for the flat circular plate, also shown on Fig. 10. If it were not for the support effect, this curve would be inversely symmetrical about the 90° angle. While the general shape exhibits such symmetry, the lack of comparison in magnitude permits an evaluation of the support interference.

While not illustrated, the axial force (parallel to the ground and in the reflector azimuth direction) exhibits relatively little change for the different

reflector focal lengths. As might be expected, the peak forces perpendicular to the paraboloid centerline are approximately 55% greater for the deepest than for the shallowest paraboloidal reflector.

D. Angular Rotation Center Location

The reflector angular positioning mechanism must be capable of overcoming the torques due to wind loads. As Fig. 11 shows, the magnitude of these torques is affected by the relative position of the moment center. For this solid-surface reflector, the peak-positive yaw moment is reduced 29% for a moment center travel equalling 30% of the diameter. The minimum yaw moment would be obtained with the moment center appreciably on the concave side of the paraboloidal reflector. With the exception of this figure, all moment curves presented in this paper are taken about the paraboloid vertex, i.e., the intersection of the paraboloid centerline and its reflecting surface.

E. Effects of Pitch Angle on Moments and Forces

Figure 12 shows an example of the variation of yaw moment vs yaw angle as a parametric function of pitch angle for a typical solid surface reflector. With the exception of lift and pitch moment, the forces and moments show peak values near zero pitch angle; the lift and pitch moment show peak values at approximately 60° pitch angle.

F. Uniformly Distributed Porosity

Figures 13 and 14 show the effect of uniformly distributed porosity on axial force and yaw moment. This effect of uniform porosity is the strongest

influence noted throughout the test; 50% porosity reduces the yaw moment positive-peak (about the vertex) 25%, eliminates any negative yaw moment, reduces the rate of change of moment with angle 84%, the peak axial force by 50%, and the peak lift (at 60° pitch angle) 80%. Some of these reductions would be even more significant in percent, as the moment center moved away from the paraboloid focal point. It is interesting to note that these reductions are approximately linear with porosity up to 25%, but the additional reductions due to 50% porosity are only on the order of half of those due to 25%.

G. Rim Porosity

Figure 15 illustrates the effect of reflector surface porosity on the rim only, the central portion being solid. While the reduction in forces and moments is smaller than that for the uniformly distributed porosity for the same total amount of porosity, the effect is slightly larger when it is distributed at the edges only. There appear to be other advantages outside of wind loads, which may result from distributing the porosity at the edges only.

H. Spoilers

Two types of protuberance spoilers were investigated. One consisted of a cowl-ring around the reflector periphery; relative to the no spoiler configuration, it did not significantly reduce the moments and it increased the forces slightly. As shown by Fig. 16, trip-fence spoilers had a beneficial effect. The larger of these two tested, having a height of 4% of the reflector diameter, reduced the peak yaw moment approximately 9%, the peak axial force 9%, and the maximum rate of change of moment with angle 17%. This particular

13

configuration was the only one tested which showed hysteresis in force or moment vs angle; the hysteresis loop occurring in yaw moment at about a 95° angle to the wind.

It is interesting to note that test data exist and at least one full size antenna is in use incorporating trip-fence spoilers having a height on the order of 10% of the reflector diameter (see Bibliography.)

I. Reflector Support Structure

Figures 17 and 18 show the effect of a simulated structural support (illustrated in Fig. 3) behind the otherwise relatively thin paraboloidal reflecting surface both with and without aerodynamic counter-balancing surfaces (extended counterweight side surface areas.) Even with the minimum size counterweights, the structure reduces the peak yaw moment about the vertex approximately 18%, apparently by yielding some aerodynamic counter-balancing. This reduction in yaw moment is obtained, however, at the expense of increasing the side force by 50%. Note that the position of the moment center will have a strong influence on the gain, due to such counter-balancing. The axial force is not significantly changed.

The simulated reflector support structure was fabricated mainly from 1/8-in. square members, in order to minimize the Reynolds number effects (as indicated by Fig. 7 for sharp edged shapes.) No check was made on the Reynolds number sensitivity of these configurations. It is realized that this model structure has fewer members of a larger relative size than most full-scale installations. Fabrication costs prohibited a more detailed model for this phase of the investigation; however, the results should be at least indicative.

Some care must be taken in designing the support for large antennas where structural members of circular cross-section are utilized. Wind-excited periodic vibrations in such members have produced structural failures on several existing installations. This phenomenon is relatively well understood, however, and is predictable (see Ref. 2.)

J. Complete Configuration

Figures 17, 18, and 19 serve to illustrate the forces and moments on one of the several possible complete configurations tested. A simulated complete configuration represented by these figures is illustrated in Fig. 3 and incorporates the rim porosity, pylon, paraboloidal reflecting surface supporting structure, and extended counterweight side surfaces. Although the yaw moment for this combination is on the order of half of that for the simple solid reflector, the side force is nearly doubled. It remains to be investigated whether or not this is a desirable compromise when compared to structural problems, angular positioning problems, etc.

K. Pressure Distribution

Figure 20 shows one of the models on which pressure distribution was measured, and Fig. 21 and 22 present samples of pressure-difference contours across a solid reflecting surface paraboloidal antenna. It is interesting to note that the pressure drops off somewhat near the edge of the reflector--a feature beneficial to reflecting surface elastic deformations caused by wind loads. These reflectors have a focal length to diameter ratio of 0.33.

15

L. Dynamic Oscillation Data

Figure 5 shows the strain gauges attached to the model support staff from which the dynamic data were obtained. These data, recorded as oscillograph traces, have not been completely reduced to date and are not presented.

SUMMARY

Only a small but most significant portion of the results of this test has been presented in this paper. These results indicate the significance of the proper design consideration of wind loads on structures of this type.

A larger and more complete report on the results of this investigation, including comparisons with data from other sources, is in preparation. Complete tabular data and a large number of working plots, in several different axes orientation systems, are available. This material can be supplied on specific request for those interested in particular features of these tests.

The material in this paper is also being presented in the JPL Space Programs Summary, 37-14, Vol. 1, I, B-2.

REFERENCES

1. PROJECT DESCRIPTION, ADVANCED ANTENNA SYSTEM FOR THE DEEP SPACE INSTRUMENTATION FACILITY, Engineering Planning Document No. 5, Rev. 1, Jet Propulsion Laboratory, 12 Oct. 1960.

2. W. Weaver, Jr., WIND-INDUCED VIBRATIONS IN ANTENNA MEMBERS, J. of Eng. Mech. Div., Proc. Am. Soc. Civ. Eng., Feb. 1961, pp. 141.

3. Sighard F. Hoerner, FLUID-DYNAMIC DRAG, Published by the author, 1958 (Lib. of Congress Cat. Card No. 57-13009).

BIBLIOGRAPHY

The following list presents several other sources of information that have come to the authors' attention, which may be of use in connection with the wind load design of paraboloical reflector antennas. In some cases, this information is unpublished, proprietary, or classified, and may not be generally available. The authors' comments on the information contained therein are included in parentheses.

1. G. K. Bentley: PARABOLIC SCANNER MODELS, Wind Tunnel Report 993, Lincoln Laboratory, Massachusetts Institute of Technology, March 1960. (Tests on a 30 in. diam. pedestal-mounted model with both solid and 62% porous surfaces, force-moment data only.)

2. H. C. Husband: THE JODRELL BANK RADIO TELESCOPE, Paper No. 6270, Procedures of the Institution of Civil Engineers, Vol. 9, p. 65, Jan. 1958.
(A general discussion on the design and fabrication of the 250 ft diam solid-surface antenna, with one yaw moment curve taken from wind loads on the completed structure.)

3. H. D. Tissue: WIND TUNNEL TESTS OF AN 0.048 SCALE MODEL OF THE M-286 RAYTHEON "PINCUSHION" RADAR ANTENNA, Report No. FWR-8, Fairchild Aircraft and Missiles Division, Hagerstown 10, Maryland, June 1960, with revision dated Nov. 1960.
(Force-moment data on a 34.5 in. diam. solid surface paraboloidal reflector with an equipment house attached to the convex surfaces, in a 38 x 54 in.

RECORDED No. 62-109

wind tunnel; partial force-moment data on a paraboloidal reflector with and without a center hole, plus pressure distribution data.

4. ANTENNA WIND LOAD TEST, Model AT-36, Dynatronics, Inc., 6 June 1961.
(Azimuth and Elevation Torques from motor current on a 60 ft diam. porous surface antenna.)

5. A. W. Sherwood, WIND-TUNNEL TESTS OF THE MARK 19 ANTENNA MOUNT WITH THE MARK 28 AND MARK 34 RADAR ANTENNAS, Report R-322, David Taylor Model Basin, Washington, D.C., Feb. 1947.
(Full scale tests to two small fire-control antennas, one porous and one solid surface.)

6. LIFT AND DRAG COEFFICIENTS FOR VARIOUS TYPES OF RADAR ANTENNA SCREENS, Report R-293, David Taylor Model Basin, Washington, D.C., Feb. 1951.
(Tests of flat screen panels typical of porous surfaces of antenna reflectors.)

7. J. B. Teideman, WIND TUNNEL STUDIES ARE MADE ON PARABOLAS, Electronics Magazine, p. 64.

8. D. W. Rinkoski and H. F. Fritsch, Jr., WIND TUNNEL TESTS ON RADAR ANTENNA SCREEN MATERIALS, DGAI Report No. 155, The Daniel Guggenheim Airship Institute, The University of Akron, Oct. 1955.
(Tests of flat screen panels typical of porous surfaces of antenna reflectors including Reynolds number effects.)

9. D. W. Rinkoski and H. F. Fritsch, Jr., WIND TUNNEL TESTS OF A 1/12 SCALE MODEL FPS-3/MPS-7 ROTATING RADAR ANTENNA, DGAI

Report No. 158, the Daniel Guggenheim Airship Institute, The University of Akron, March 1949.

(Moment data only on a porous surface antenna with an eliptical, rather than circular, peripheral shape.)

10. W. G. Raymer and H. L. Nixon, AERODYNAMIC TESTS OF A MODEL OF A RADIO TELESCOPE, PART I. MEASUREMENT OF THE STATIC WIND FORCES, NPL/Aero/275, National Physical Laboratory, Rev. Nov. 1961.
(Force and moment data on a 2.5 ft diam. solid-surface model, cradle mounted. Also contains some dynamic stability data.)

11. D. H. Williams, H. L. Nixon, and W. C. Skelton, TESTS ON MODELS OF PARABOLIC REFLECTORS FOR THE DECCA RADAR CO., LTD., NPL/Aero/250, National Physical Laboratory, Rev. Nov. 1961.
(Two force and one moment data on 3.2 ft diam solid- and slatted-surface models without a ground plane.)

12. Reports from GALCIT Test No. 714, 734, and 737 performed in March, Sept., and Dec. 1958 for the Philco Corp. WDL.
(Force and moment data on a 2 ft diam. solid-surface model with enclosed structural support without a ground plane and spoilers not currently available to the author.)

13. Report from Ames Aeronautical Laboratory Test No. 7-34 in the 7 x 10 ft tunnel, performed in Feb. 1962.
(Force and moment data plus pressure distribution data, on a 2 ft diam. solid-surface model with enclosed structural support, with and without spoilers. Not currently published.)

NOMENCLATURE

Model Attitude

The position of the paraboloidal reflector, relative to the wind, is defined by the yaw and pitch angles. In astronautical parlance, these are known as the azimuth and elevation angles, respectively. Yaw angle is the angle between the wind and the centerline of the paraboloidal reflector about an axis parallel to the force of gravity. Pitch angle is the angle between the wind and the centerline of the paraboloical reflector about an axis perpendicular to the force of gravity and the model axis of symmetry. When both the yaw and pitch angles are zero, the concave side of the reflector is directed symmetrically upwind. When the pitch angle is 90°, the generating centerline of the reflector is parallel to gravity and the antenna is pointed at the zenith.

Axes Systems for Forces and Moments

The forces and moments caused by wind loads may be expressed in any one of three orthogonal cartesian coordinate systems whose angular orientation is defined as follows:

Wind Axis: An axis system which is always parallel to the ground surface, the wind direction, and the direction of gravity (the ground surface is assumed to always be flat and level.)

Body Axis: An axis system which is always parallel and perpendicular to the axis of symmetry of the model body (paraboloidal generating centerline.) In the

particular case of this test, the side force is also parallel to the ground surface as there is no roll angle.

Stability Axis: An axis system which is parallel to the ground surface and the direction of gravity but is perpendicular to the model axis of symmetry. (And therefore not necessarily parallel to the wind direction.)

Note that all three of these axes systems are coincident when the yaw and pitch angles are zero. Of these three axes systems, data in the stability axes are probably the most applicable to an Az-El mounted antenna; none of these axes systems are directly applicable to a Ha-Dec mounted antenna, where the orientation is determined by the Earth's rotational axis rather than the local direction of gravity.

Moment Centers

The position of the center of moments for the data presented in this paper is always on the paraboloidal surface generating centerline. Its position on this centerline is measured in reflector diameters forward (concave side) or aft (convex side) from the vertex. The vertex is defined as the intersection of this generating centerline with the reflecting surface.

Force, Moment and Pressure Coefficients

The forces and moments presented in this paper are in the form of the customary nondimensional aerodynamic coefficients. The force coefficients are defined as:

$$\frac{\text{(force)}}{\text{(dynamic pressure) x (reflector frontal area)}}$$

and the moment coefficients as:

$$\frac{\text{(moment)}}{\text{(dynamic pressure) x (reflector frontal area) x (reflector diameter)}}$$

and the pressure coefficients as:

$$\frac{\text{(local surface pressure) - (ambient static barometric pressure)}}{\text{(dynamic pressure)}}$$

The ΔC_p of Fig. 21 and 22 is the difference of this pressure coefficient between the front and back surfaces of the reflector at corresponding positions. The dynamic pressure is defined as:

$$1/2 \text{ (ambient static air density) x (air velocity)}^2$$

A table of dynamic pressure covering usual wind velocities for a sea-level NACA standard day is presented for convenience:

Wind velocity mi/hr	Dynamic pressure lb/ft^2
0	0.00
10	0.26
20	1.02
30	2.30
40	4.09
50	6.39
60	9.21
70	12.26
80	16.37
90	20.71
100	25.58
110	30.94
120	36.83

23

Force and Moment Sign Conventions

As mentioned above at zero yaw and pitch angles, the three axes systems are coincident; the forces and moments in each of these systems must also be coincident and, therefore, will be defined for this condition.

Drag, chord, or axial force:	Positive in a down-wind direction or away from the convex surface of the reflector.
Lift or normal force:	Positive in a vertical direction.
Side, lateral, or span-wise force:	Positive to the right (starboard) when facing up-wind.
Pitch moment:	Positive for an up-wind or concave side of the reflector up moment.
Yaw moment:	Positive for an up-wind or concave side of the reflector to the right (starboard) moment.
Roll moment:	Positive for a right (starboard) side of the reflector down-moment (facing up-wind.)

The orientation of these forces and moments will change with the yaw and pitch angles according to the particular axis system involved.

Numerical Example

As an example of the use of these definitions, a yaw moment coefficient in either wind or stability axis with a numerical value of 0.15, when applied to a 200 ft diam.antenna in a 70 mph steady wind, yields:

$$0.15 \times 12.26 \times 31416 \times 200 = 11.6 \text{ million ft. lb. torque}$$

in a clockwise direction looking down. For this same situation, an axial force coefficient, in stability axes, of 1.60 yields:

$$1.60 \times 12.26 \times 31416 = 0.472 \text{ million lb. force}$$

acting in a direction away from the concave surface of the reflector and parallel to the ground surface.

25

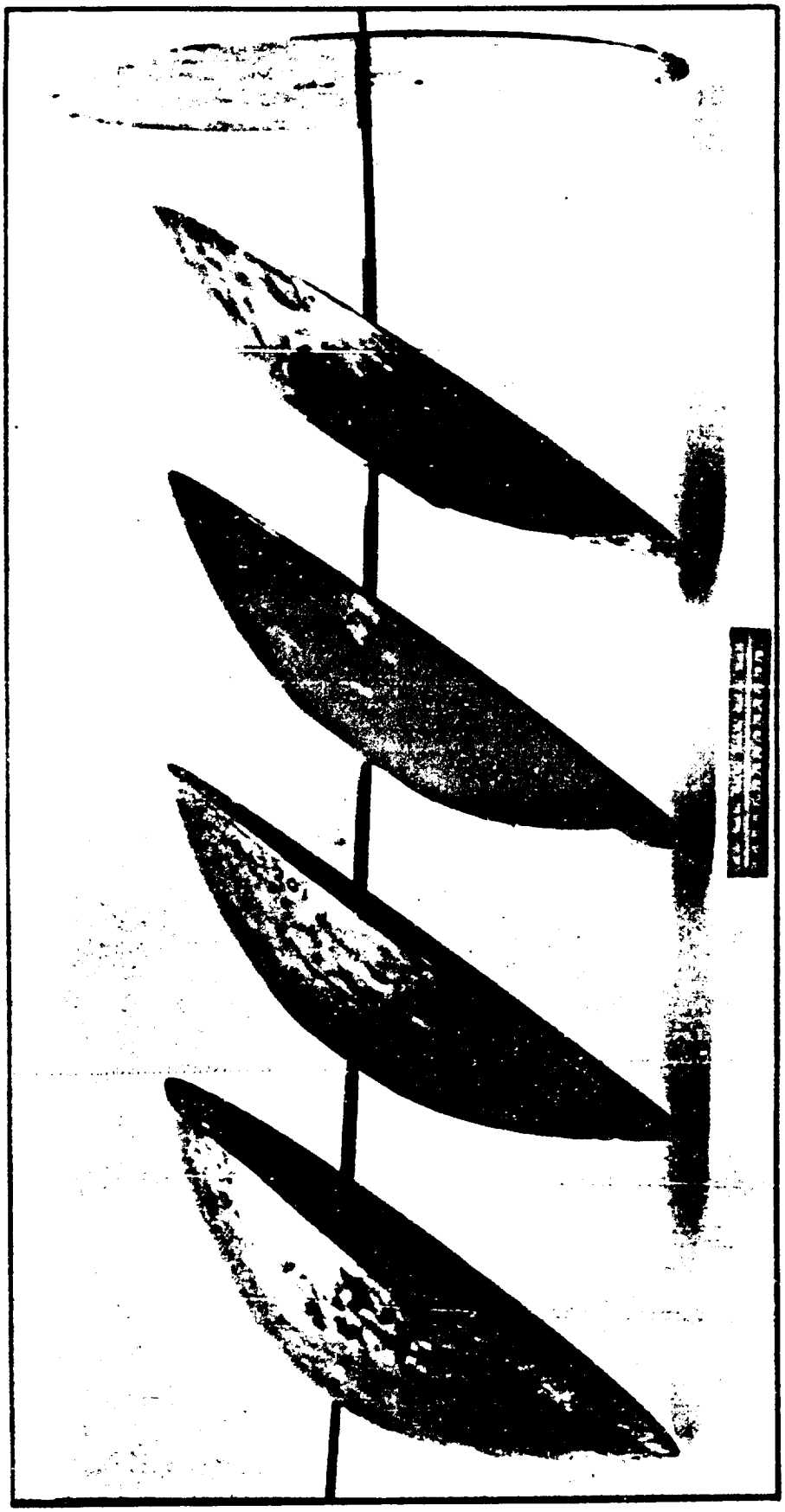

Dish depth / Diameter	Focal length / Diameter
0.250	0.25
0.215	0.29
0.189	0.33
0.149	0.42
0	∞

Antenna dishes of various depths

FIGURE 1

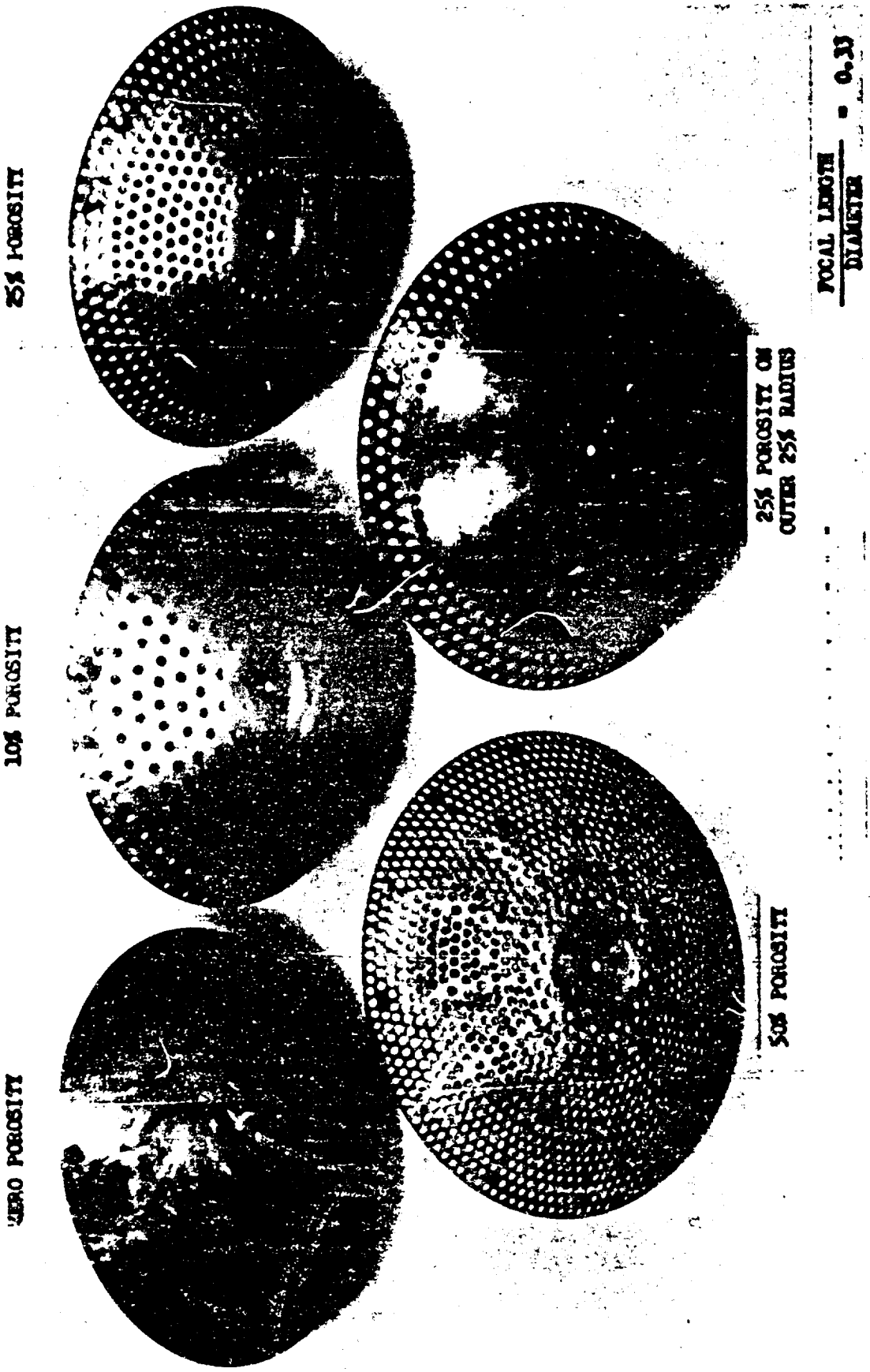

Perforated antenna dishes

FIGURE 2

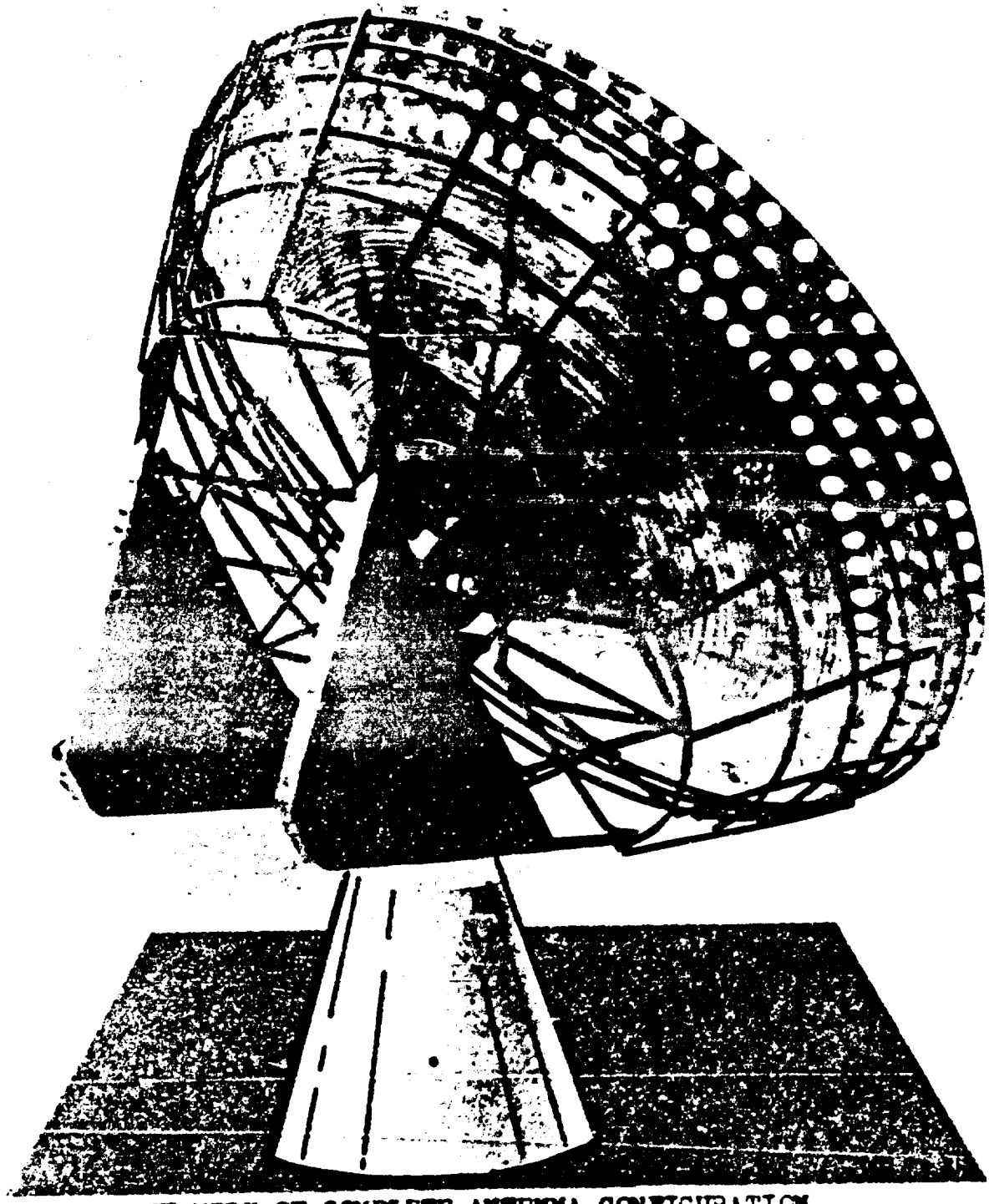

EXAMPLE OF COMPLETE ANTENNA CONFIGURATION

$\frac{F.L.}{Dia.}$ = 0.33, 25% Porosity on Outer 25% Radius

28

Enlarged counterweight side surfaces pylon mounted

FIGURE 3

Cowl ring spoiler

FIGURE 4

Fence-type spoiler

FIGURE 5

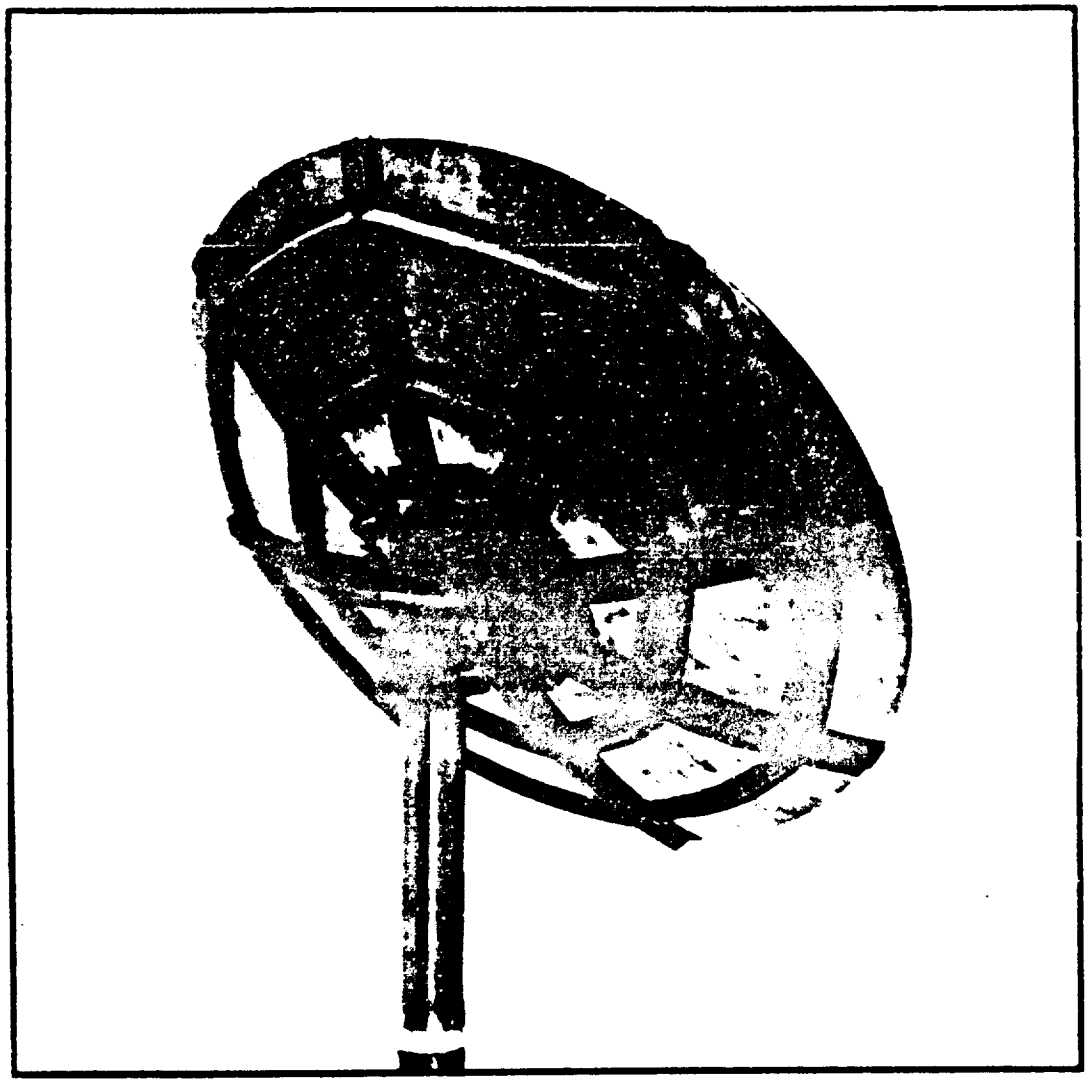

Surface roughness on convex side of reflector

FIGURE 6

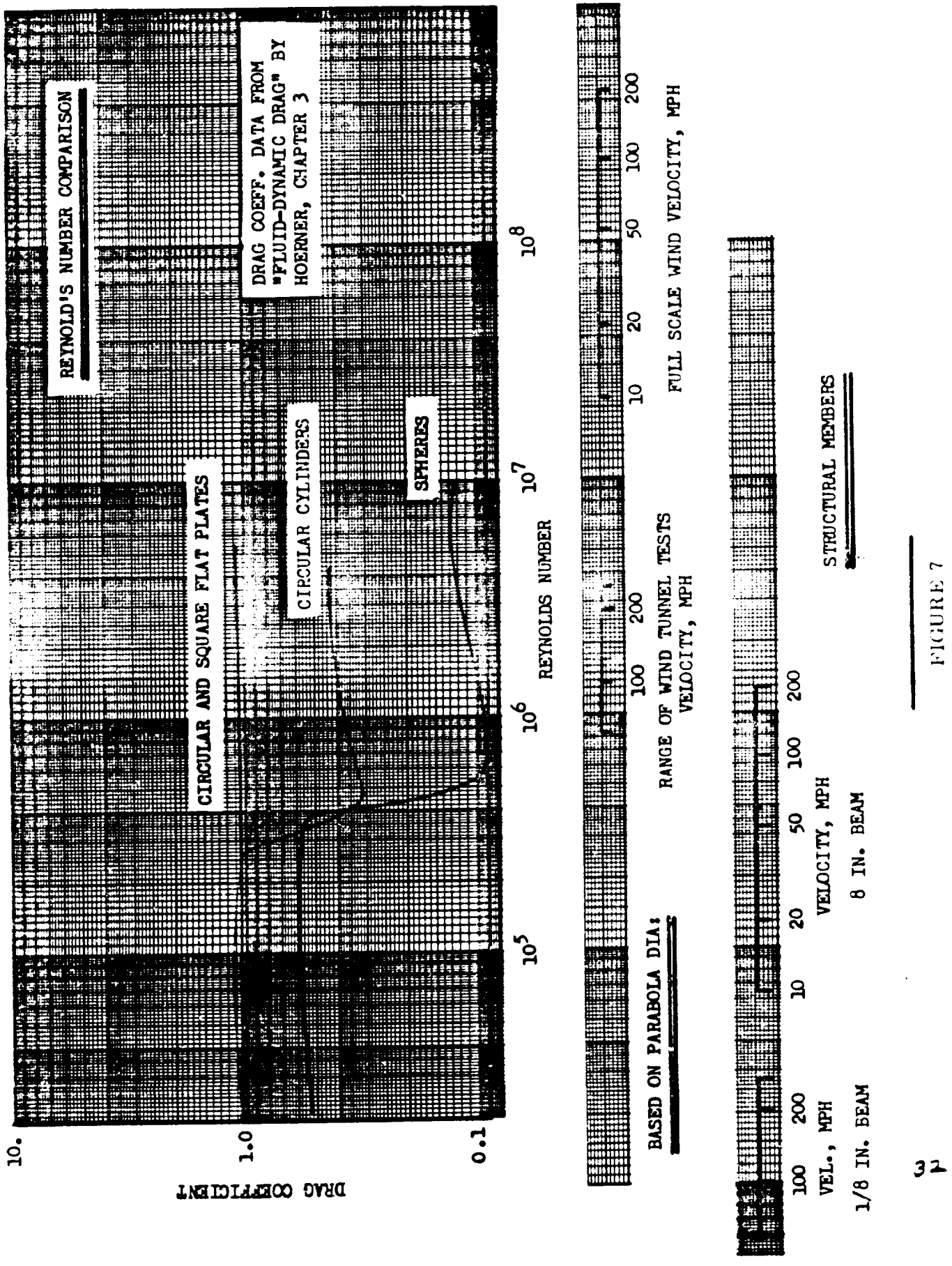
REYNOLD'S NUMBER COMPARISON
DRAG COEFF. DATA FROM "FLUID-DYNAMIC DRAG" BY HOERNER, CHAPTER 3
CIRCULAR AND SQUARE FLAT PLATES
CIRCULAR CYLINDERS
SPHERES
DRAG COEFFICIENT
10.
1.0
0.1
10^5
10^6
10^7
10^8
REYNOLDS NUMBER
BASED ON PARABOLA DIA:
RANGE OF WIND TUNNEL TESTS
VELOCITY, MPH
FULL SCALE WIND VELOCITY, MPH
VEL., MPH
1/8 IN. BEAM
VELOCITY, MPH
8 IN. BEAM
STRUCTURAL MEMBERS

FIGURE 7

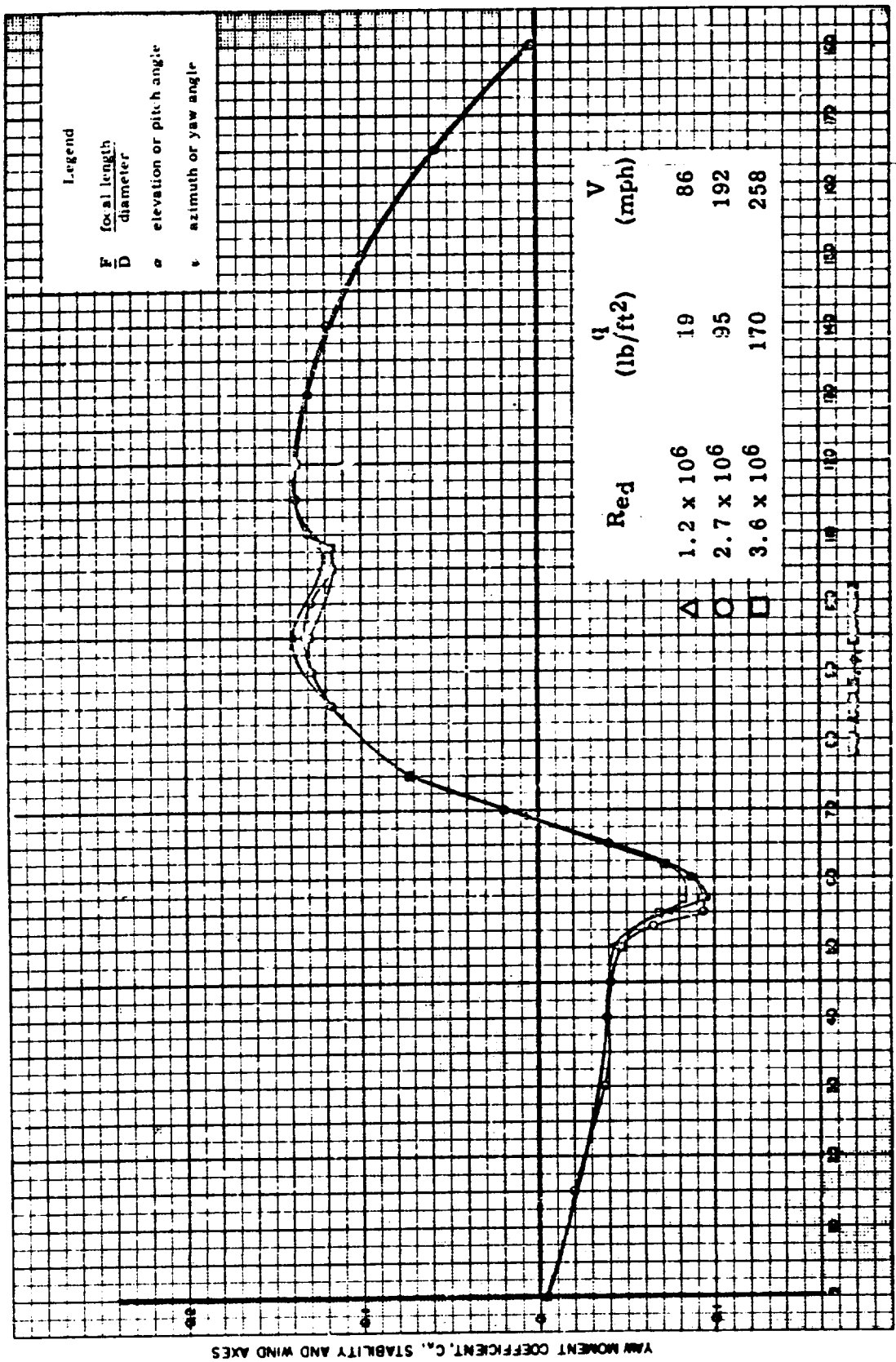

Effect of Reynolds number on yaw moment

$\frac{F}{D}$ = 0.33, zero porosity, α = 0°

FIGURE 8

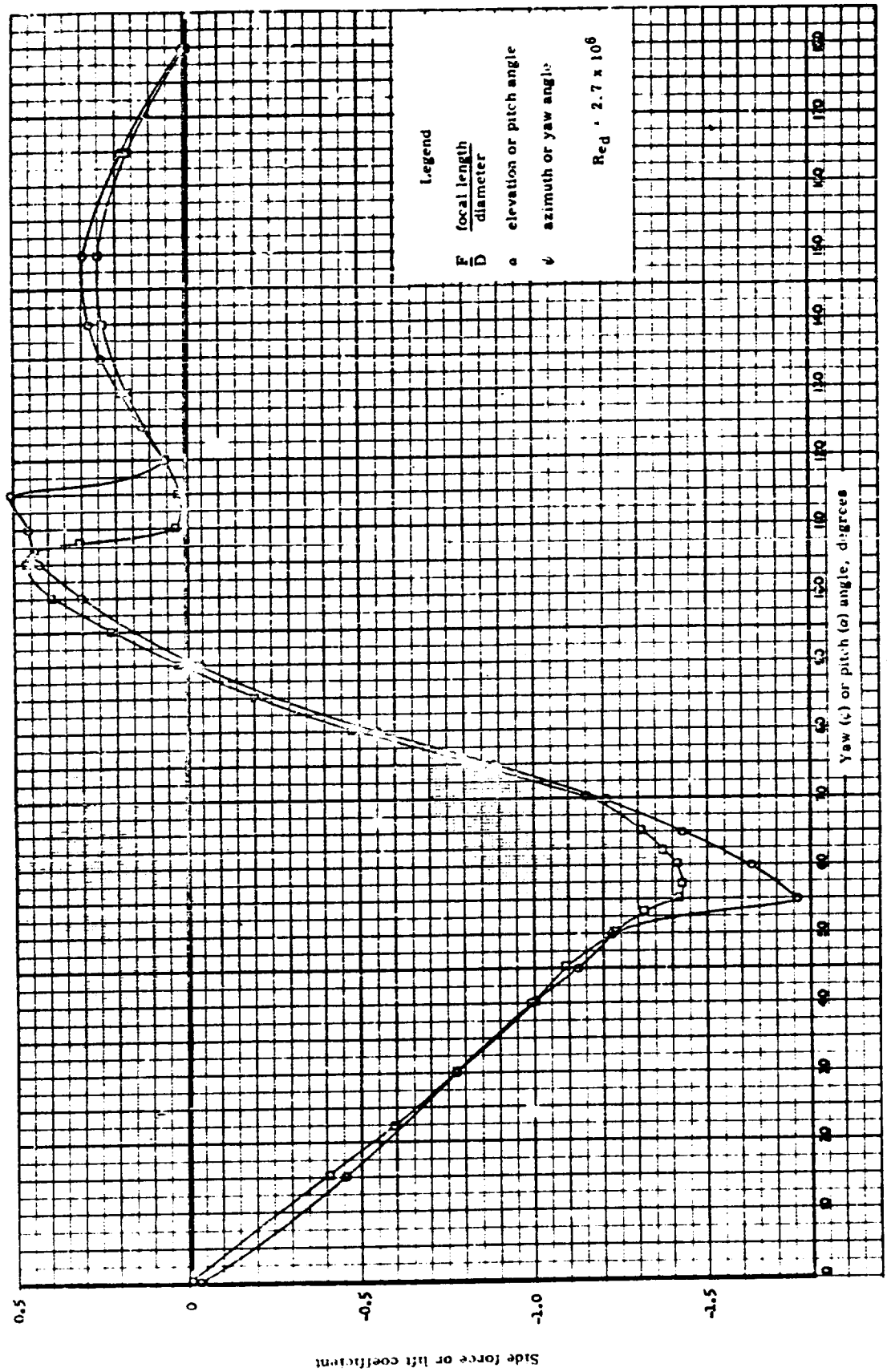

Comparison of side force (wind axes) at α = 0°, ψ variable with lift at ψ = 0° or 180°, α variable

$\frac{F}{D}$ = 0.33, zero porosity

FIGURE 6

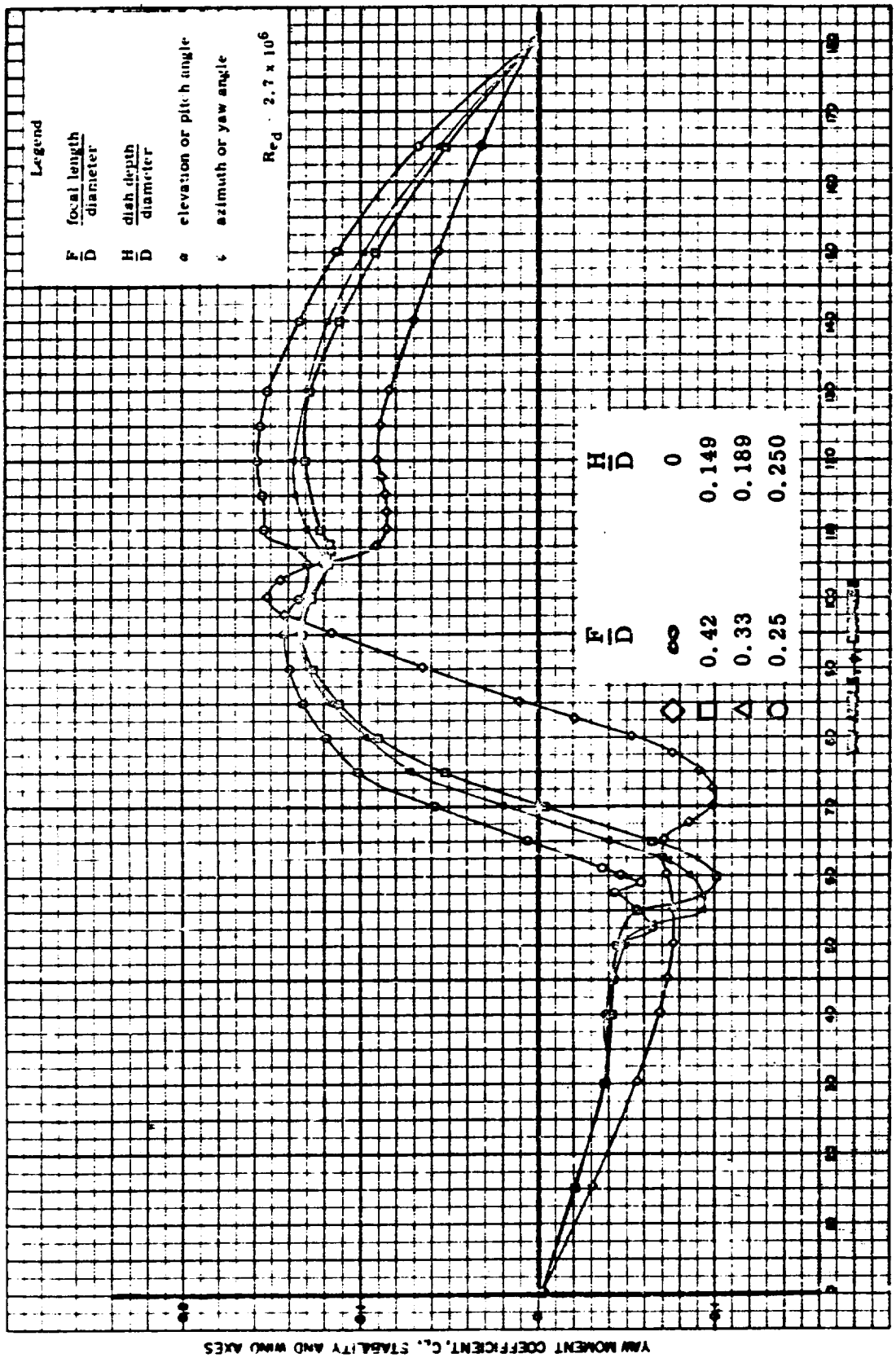

Effect of antenna dish depth on yaw moment
Zero porosity, α = 0°

FIGURE 10

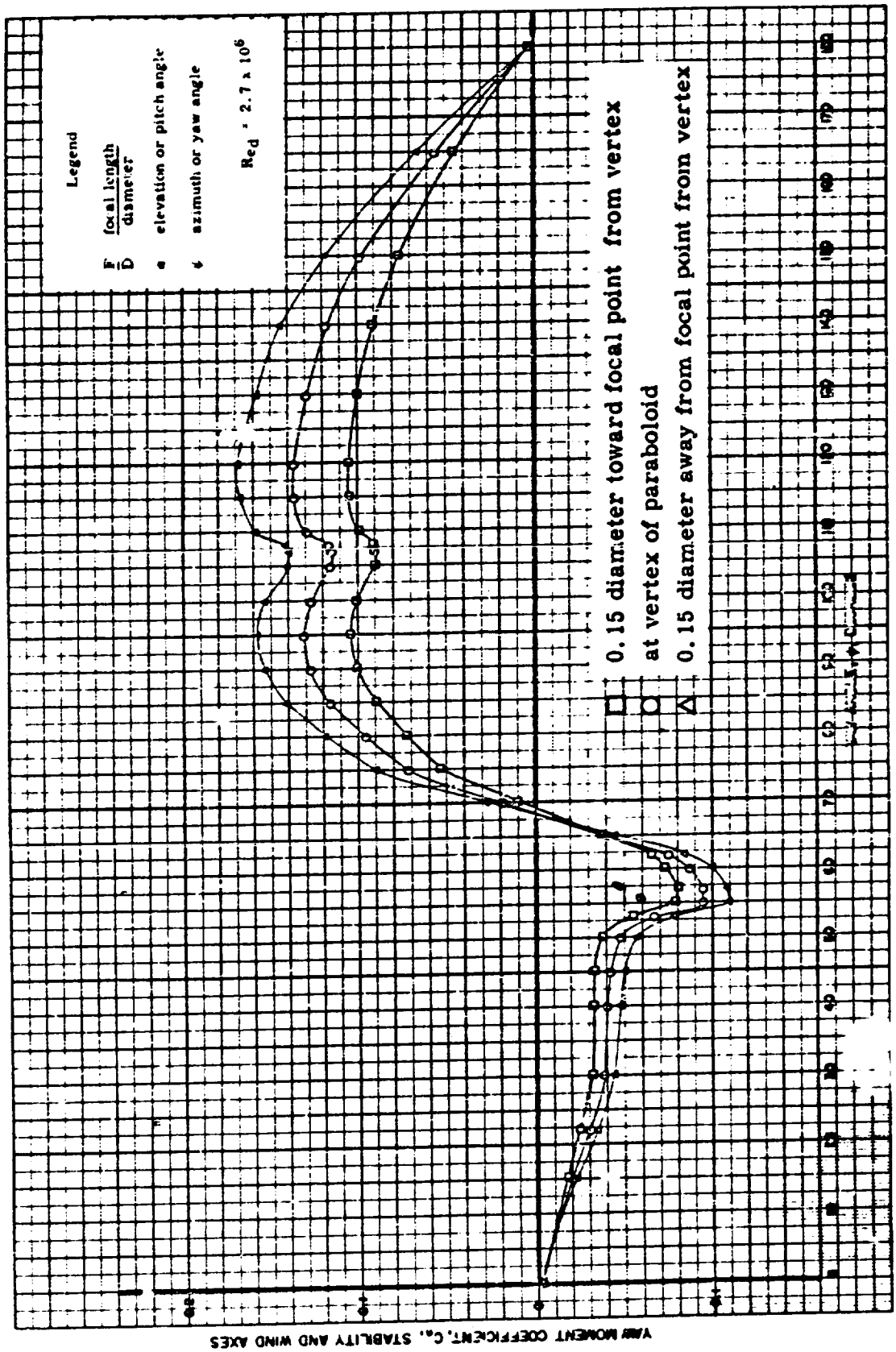

Effect of yaw axis location on yaw moment

$\frac{F}{D}$ = 0.33, zero porosity, α = 0°

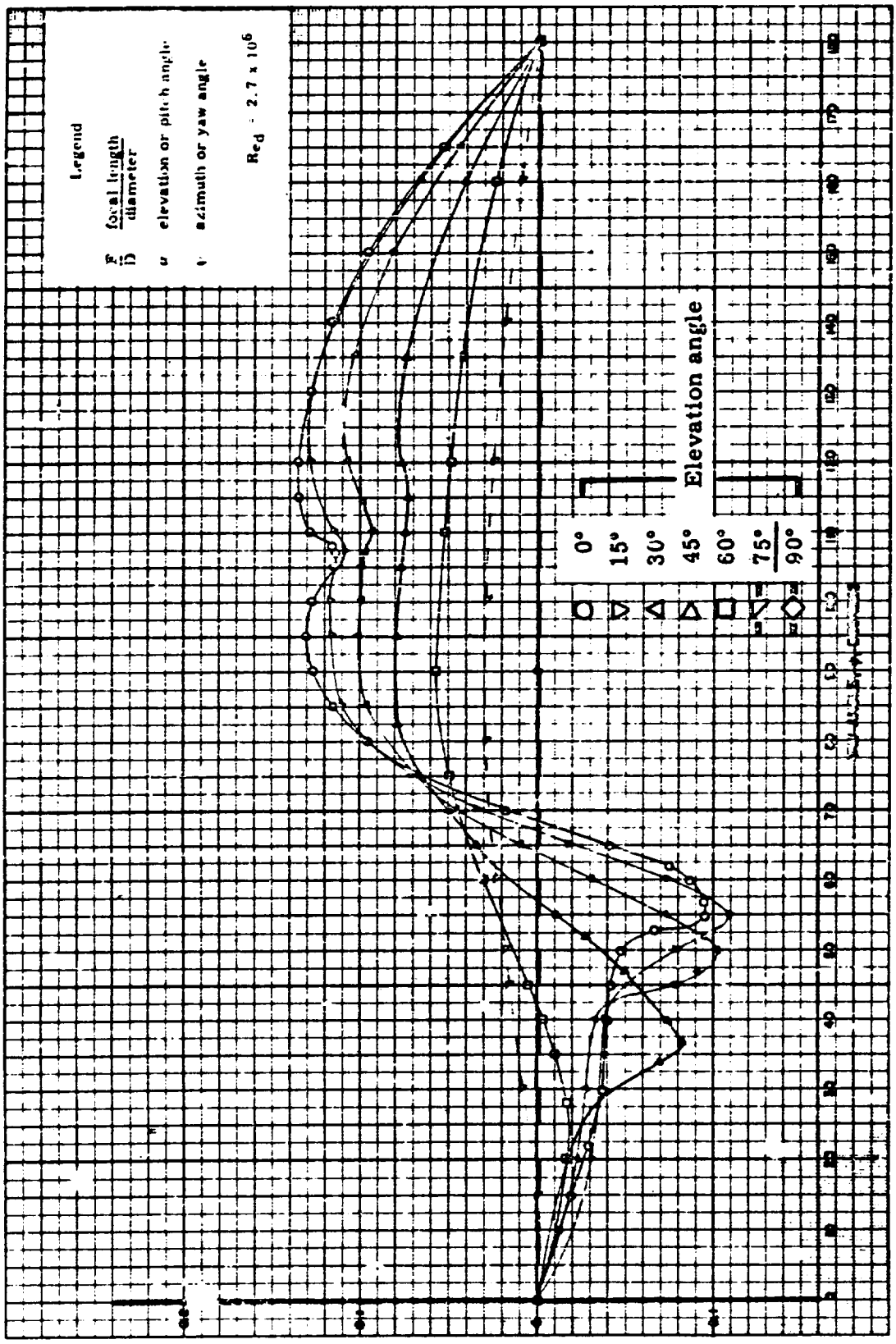

Effect of elevation (pitch) angle on yaw moment

$\frac{F}{D}$ = 0.33, zero porosity

FIGURE 12

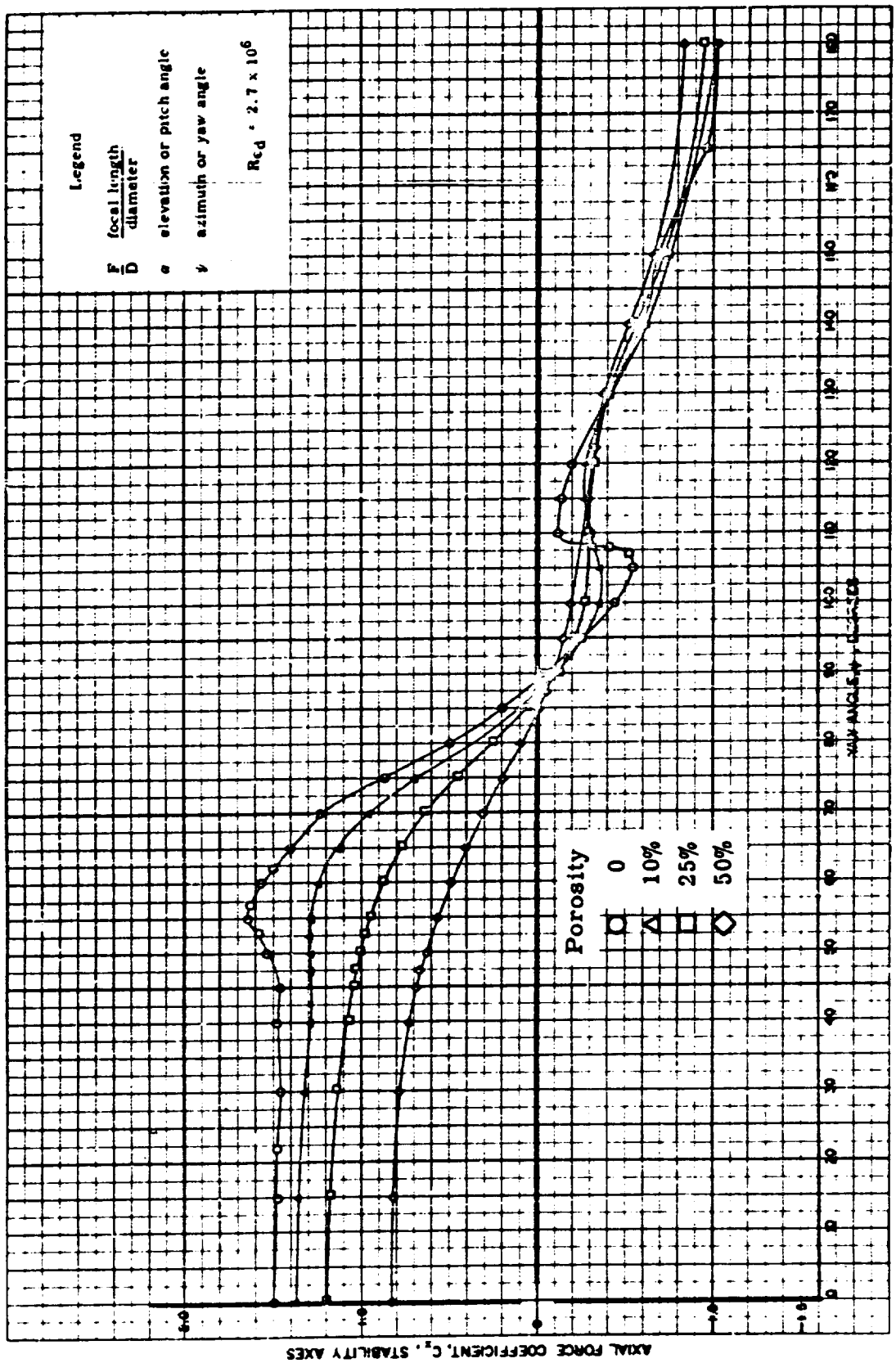

Effect of antenna dish uniform porosity on axial force

$\frac{F}{D} = 0.33$, $\alpha = 0°$

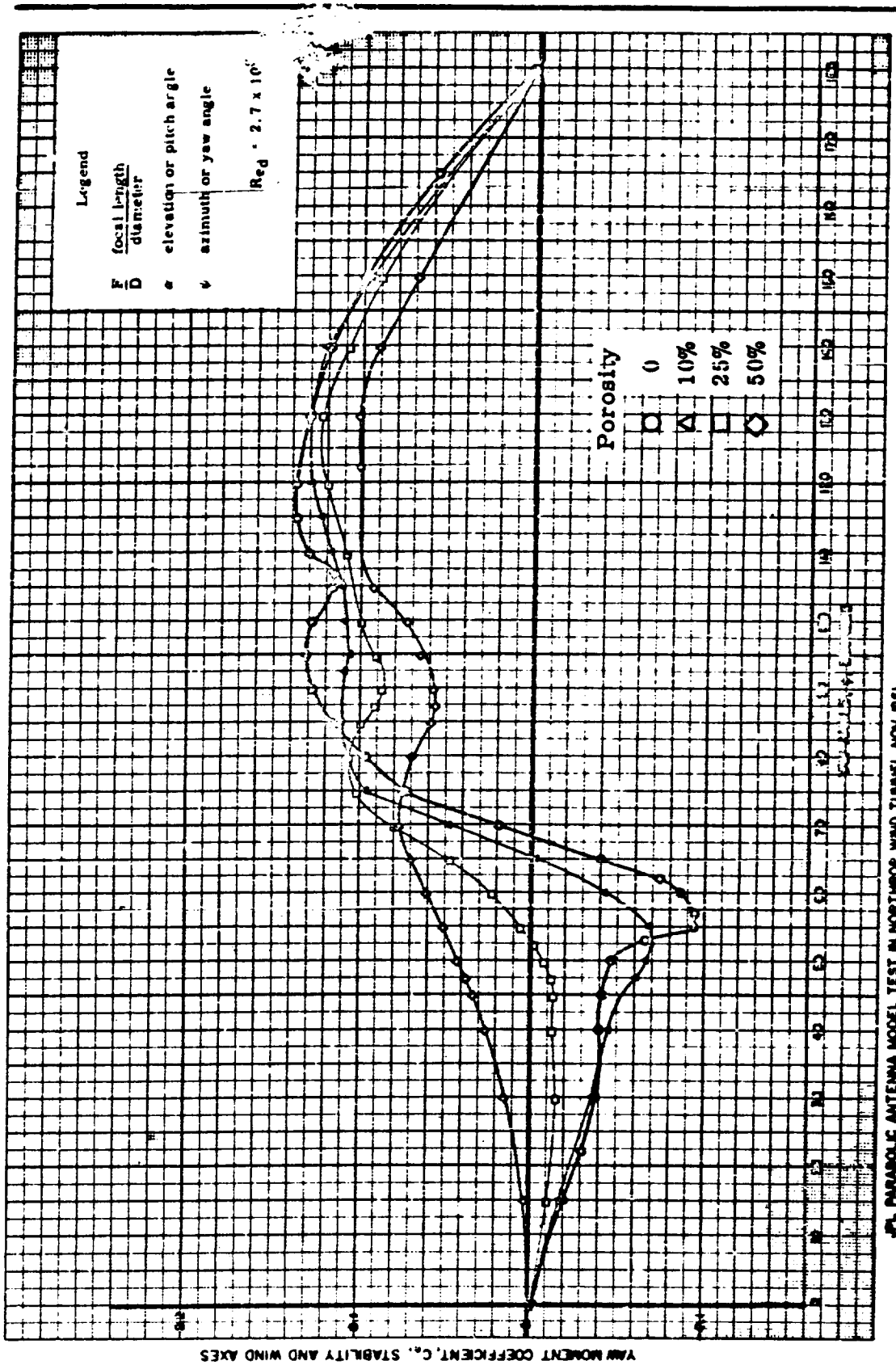

Effect of antenna dish uniform porosity on yaw moment

$\frac{F}{D}$ = 0.33, α = 0°

FIGURE 14

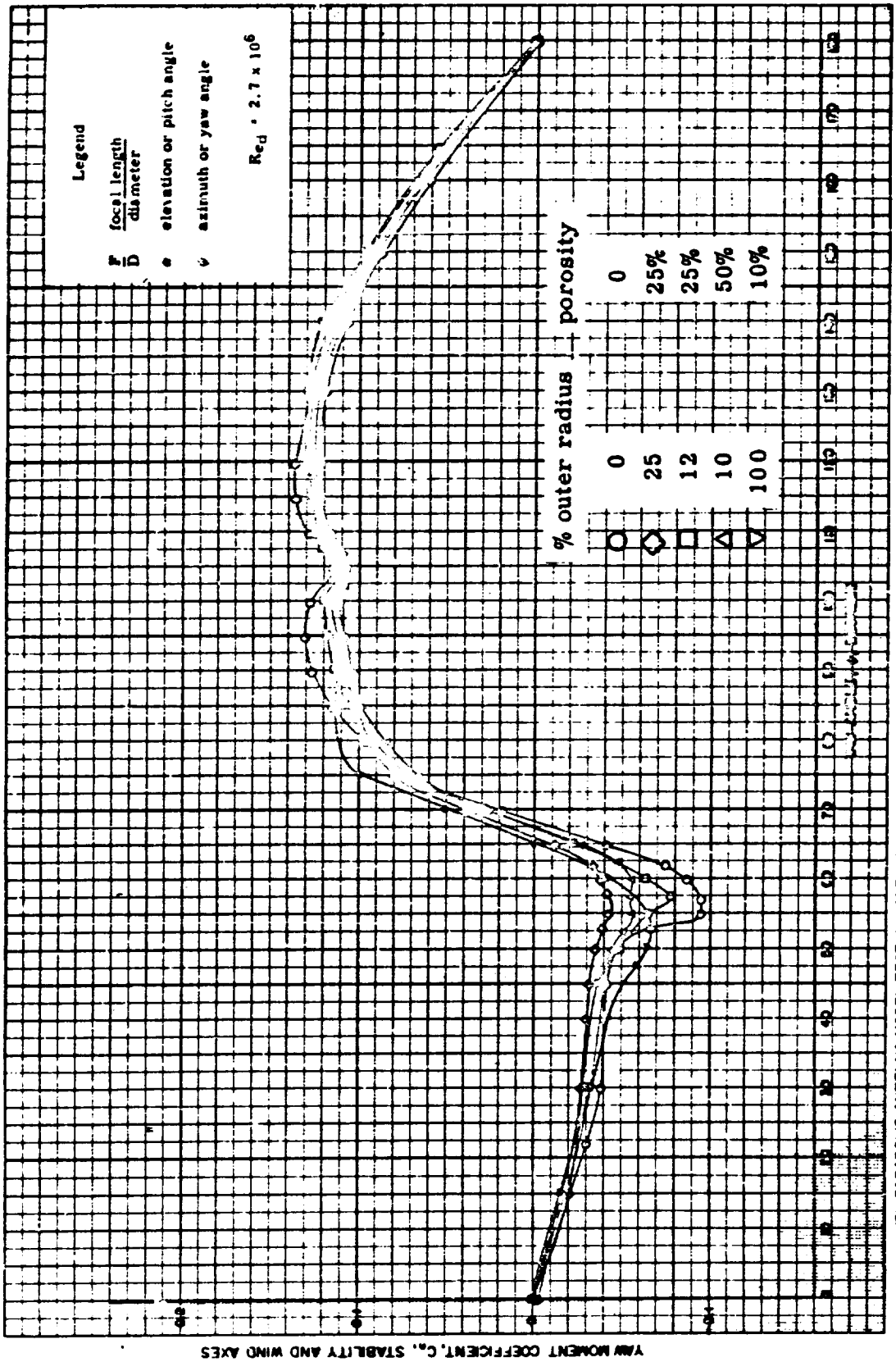

Effect of antenna dish rim porosity on yaw moment

$\frac{F}{D} = 0.33$, $\alpha = 0°$

FIGURE 15

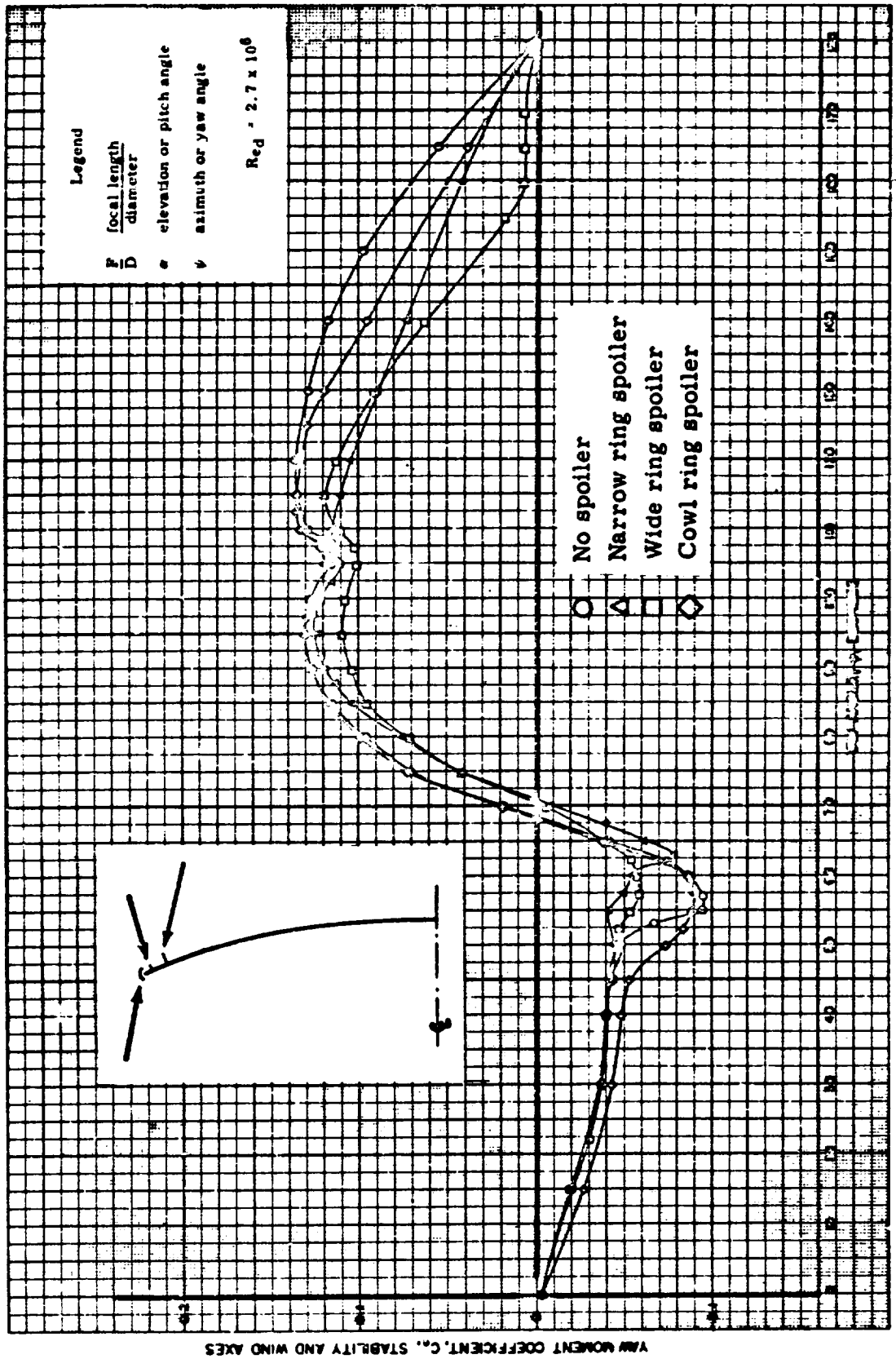

Effect of antenna dish spoilers on yaw moment
$\frac{F}{D}$ = 0.33, zero porosity, α = 0°

FIGURE 16

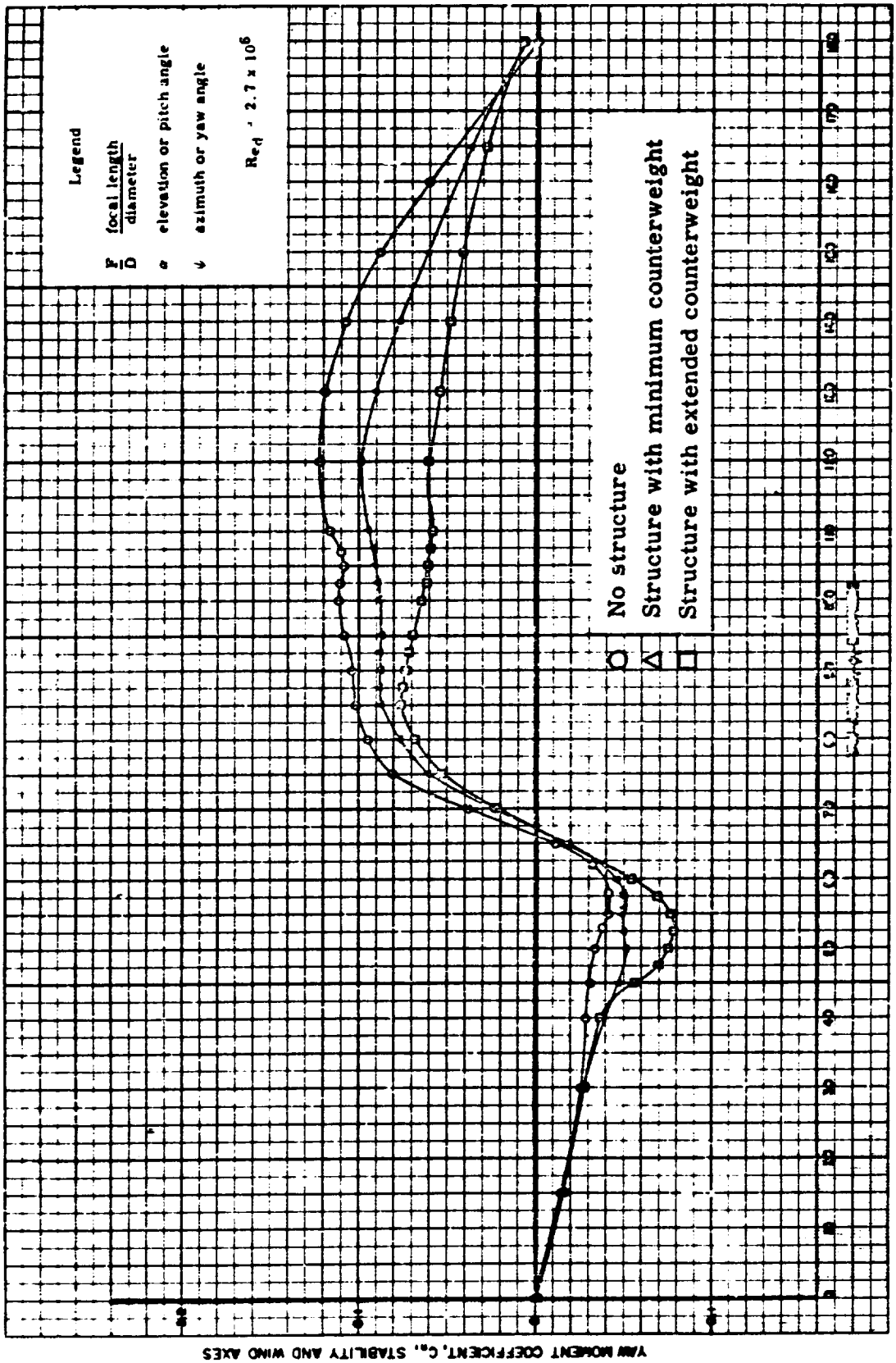

Effect of simulated structural support on yaw moment

$\frac{F}{D} = 0.33$, 25% porous on 25% outer radius, $\alpha = 0°$

Effect of simulated structural support on lateral force

$\frac{F}{D}$ = 0.33, 25% porous on 25% outer radius, α = 0°

FIGURE 18

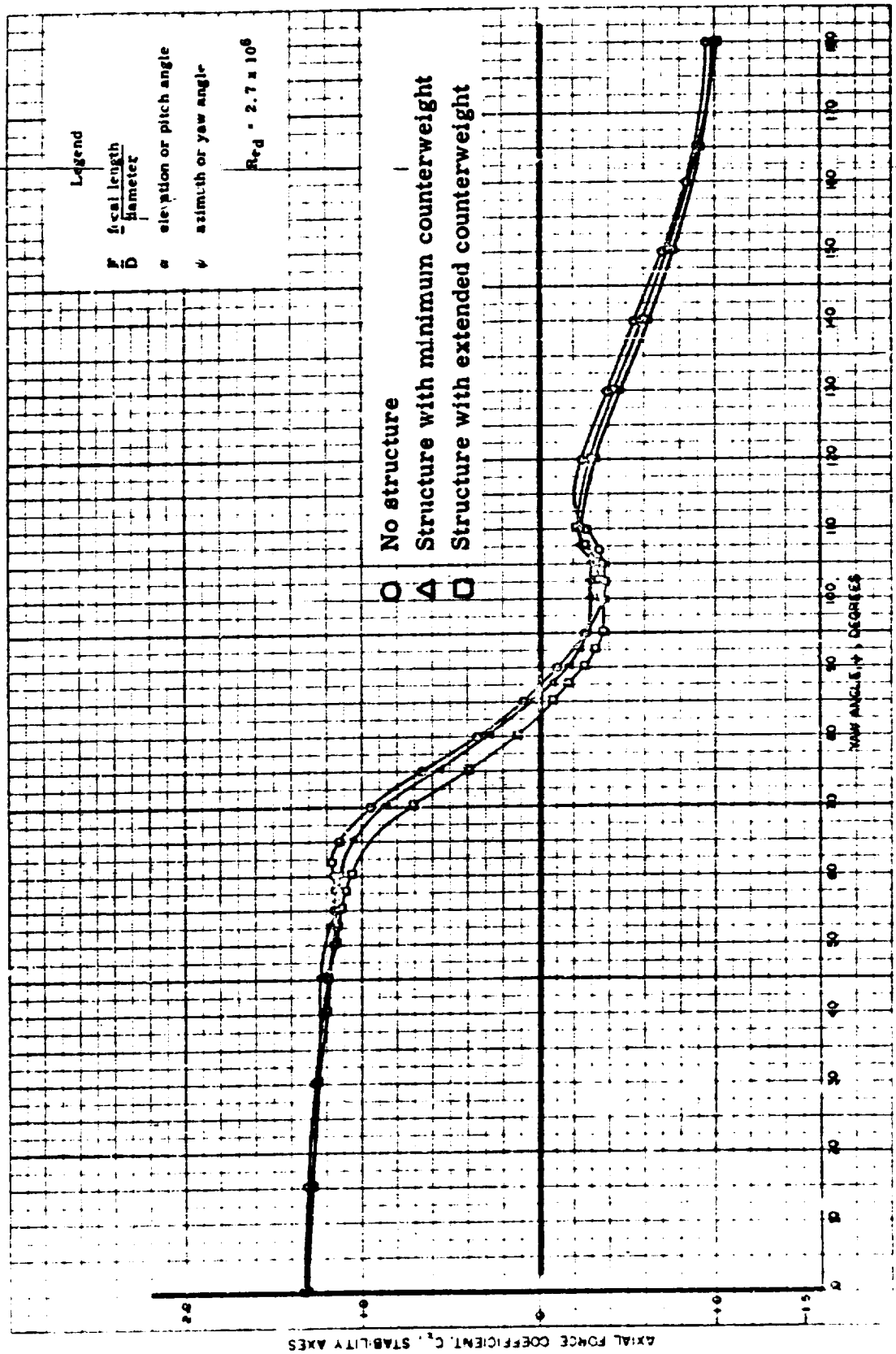

Effect of simulated structural support on axial force

$\frac{F}{D}$ = 0.33, 25% porous on 25% outer radius, α = 0°

FIGURE 10

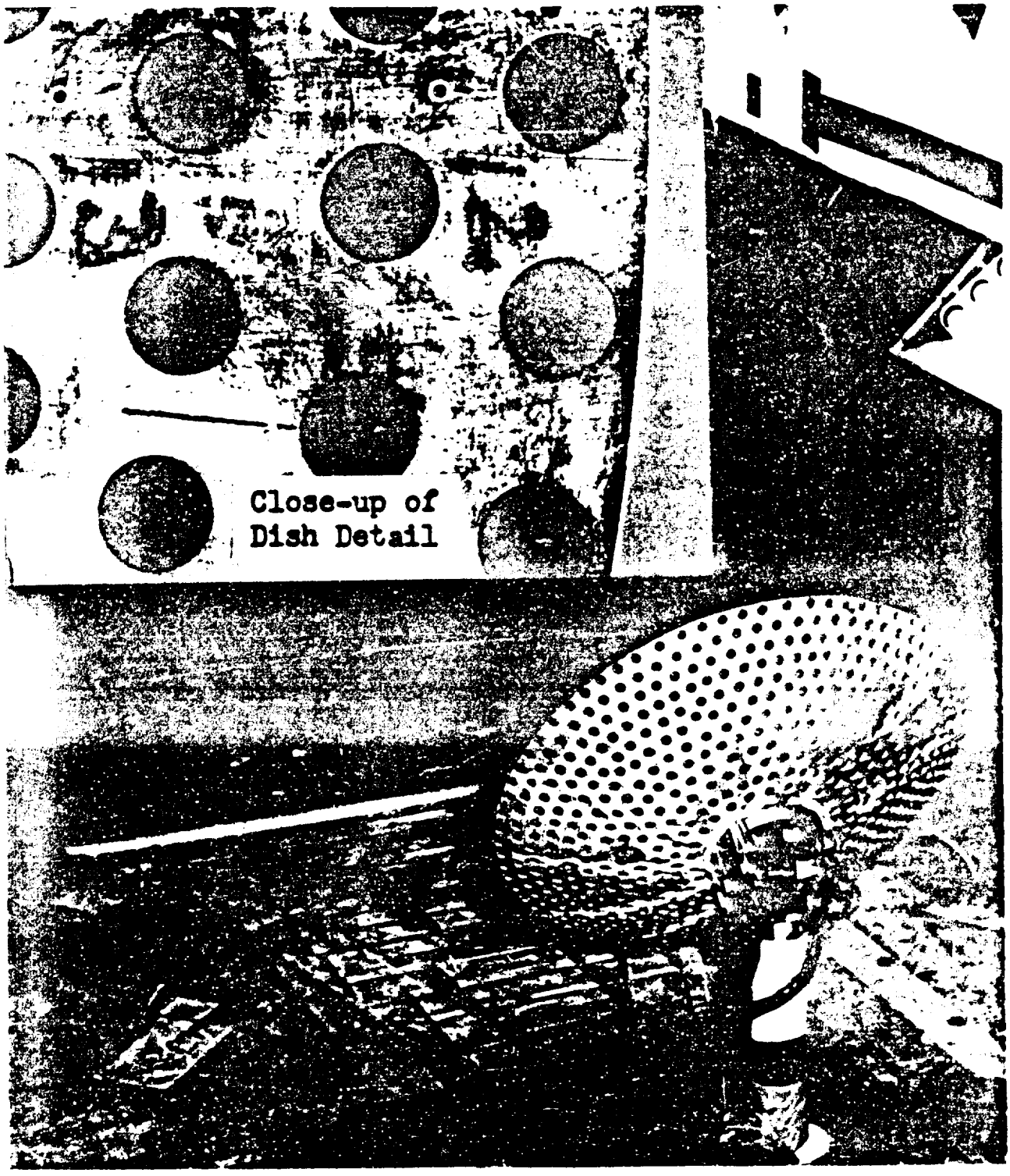

25% porosity pressure model

$$\frac{\text{F.L.}}{\text{Dia.}} = 0.33$$

FIGURE 20

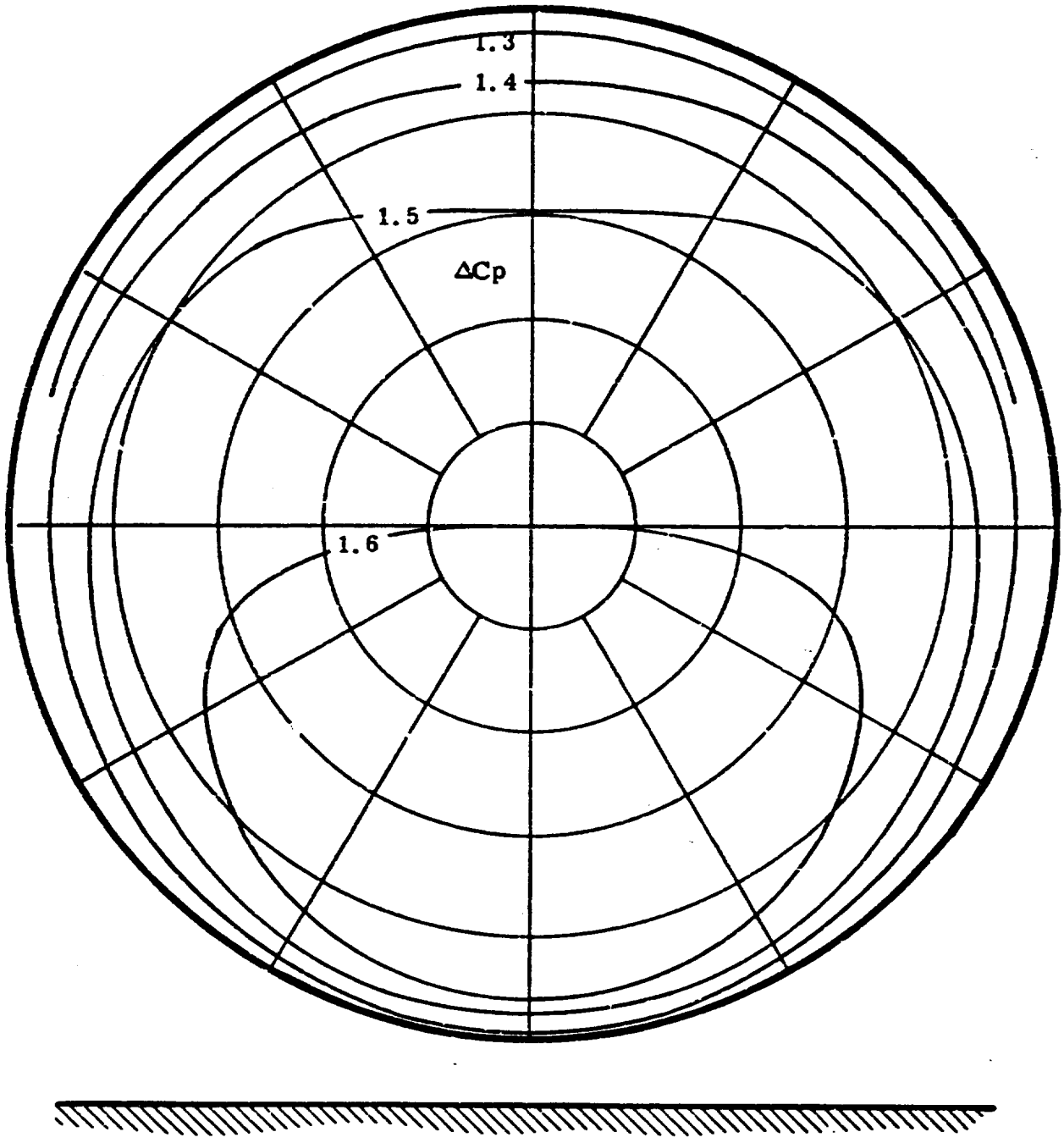

Ground Plane

Concave side of paraboloidal reflector
facing into the wind
α = zero degrees, ψ = zero degrees

FIGURE 21

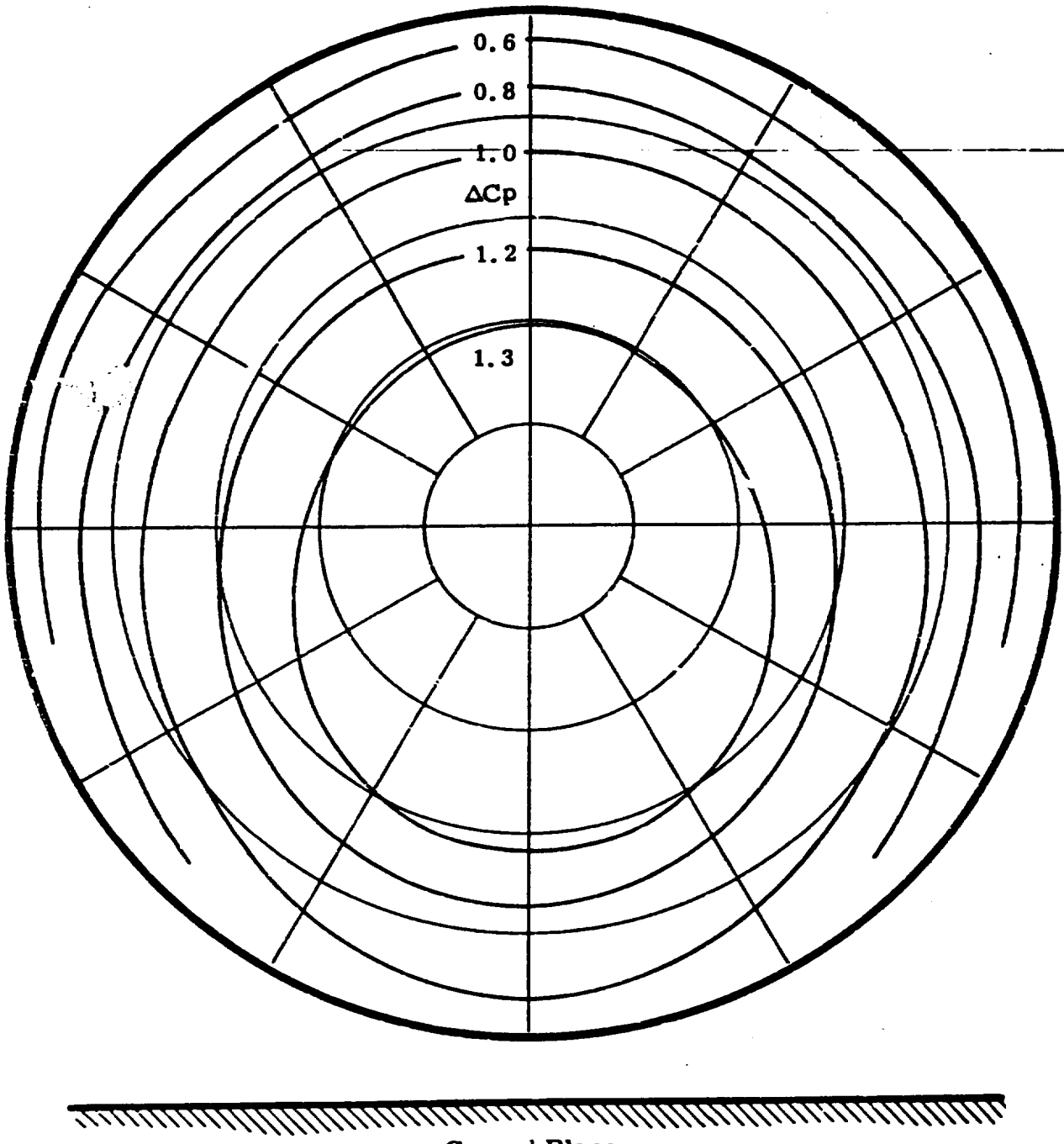

Convex side of paraboloidal reflector
facing into the wind
α = zero degrees, ψ = 180 degrees

FIGURE 22